Draft version July 1, 2019
Typeset using LaTeX **twocolumn** style in AASTeX62

The Laboratory Millimeter and Sub-millimeter Rotational Spectrum of Lactaldehyde and an Astronomical Search in Sgr B2(N), Orion-KL, and NGC 6334I

Elena R. Alonso,[1,*] Brett A. McGuire,[2,3,†] Lucie Kolesniková,[1] P. Brandon Carroll,[3] Iker León,[1] Crystal L. Brogan,[2] Todd R. Hunter,[2] Jean-Claude Guillemin,[4] and Jose L. Alonso[1]

[1] *Grupo de Espectroscopia Molecular (GEM), Edificio Quifima, Laboratorios de Espectroscopia y Bioespectroscopia, Unidad Asociada CSIC, Parque Científico UVa, Universidad de Valladolid, 47011 Valladolid, Spain*

[2] *National Radio Astronomy Observatory, Charlottesville, VA 22903, USA*

[3] *Center for Astrophysics | Harvard & Smithsonian, Cambridge, MA 02138, USA*

[4] *Univ Rennes, Ecole Nationale Supèrieure de Chimie de Rennes, CNRS, ISCR-UMR6226, F-35000 Rennes, France*

ABSTRACT

We present a laboratory rotational study of, and astronomical search for, lactaldehyde ($CH_3CH(OH)CH(O)$), one of the simplest chiral molecules that could reasonably be seen in the interstellar medium, in the millimeter and sub-millimeter wave regions from 80 to 460 GHz. More than five thousand transitions were assigned to the most stable conformer, and a set of spectroscopic constants was accurately determined. Lactaldehyde is involved in numerous metabolic pathways used by life on Earth, and is a logical step up in complexity from glycolaldehyde ($CH(O)CH_2OH$) which is being detected with increasing regularity in the interstellar medium. We present an accompanying radio astronomical search for lactaldehyde in three high-mass star-forming region (NGC 6334I, Sgr B2(N), and Orion-KL) as well as in the publicly available data from the ASAI Large Project. Neither molecule is detected in these sources, and we report corresponding upper limits to the column densities. We discuss the potential utility of lactaldehyde in combination with other members of the [C_3,H_6,O_2] isomeric family in probing pathways of chemical evolution in the interstellar medium.

Keywords: Astrochemistry, ISM: molecules

1. INTRODUCTION

To date, more than 204 molecules have been detected in the interstellar and circumstellar medium (McGuire 2018). Among these are a number of small (by terrestrial standards) organic molecules that are potential precursors to truly biologically relevant molecules such as amino acids and sugars. One of the most well-studied of these is glycolaldehyde ($CH(O)CH_2OH$), a diose and the simplest sugar-related species (Hollis et al. 2000). While searches for glyceraldehyde ($CH(O)CH(OH)CH_2OH$) – a triose and the simplest sugar – have so far failed (Hollis et al. 2004b), glycolaldehyde has been increasingly commonly observed as the sensitivity and spatial resolution of observational facilities have advanced (McGuire et al. 2018b). Searches for species with complexity in between that of glycolaldehyde and glyceraldehyde might therefore prove fruitful in understanding the lack of detection of a true sugar in the gas-phase interstellar medium (ISM). With many more members than the [C_2,H_4,O_2] family that includes glycolaldehyde, the [C_3,H_6,O_2] isomeric family may serve as a similar probe for the next step of complexity, but only if these species can be detected and studied.

Six of the lowest-energy members of this family are propionic (or propanoic) acid, methyl acetate, ethyl formate, hydroxyacetone, lactaldehyde, and methoxyacetaldehyde (Figure 1). Methyl acetate and ethyl formate have been detected in the interstellar medium (Tercero et al. 2013; Belloche et al. 2009; Peng et al. 2019), while non-detections have been reported for hydroxyacetone (Apponi et al. 2006) and methoxyacetaldehyde (Kolesniková et al. 2018). Of the remaining two, laboratory mm-wave spectra spectra exist for propionic acid (Stiefvater 1975b,a; Jaman et al. 2015). The rotational spectrum of lactaldehyde ($CH_3CH(OH)CH(O)$) has not been reported in the literature, making an interstellar search impossible. Lactaldehyde is essentially glycolaldehyde that has been substituted by a methyl group on the hydroxyl carbon (Figure 2), with sub-

* Current address: Biofisika Institute (CSIC, UPV/EHU), Bilbao, Spain.

† B.A.M. is a Hubble Fellow of the National Radio Astronomy Observatory.

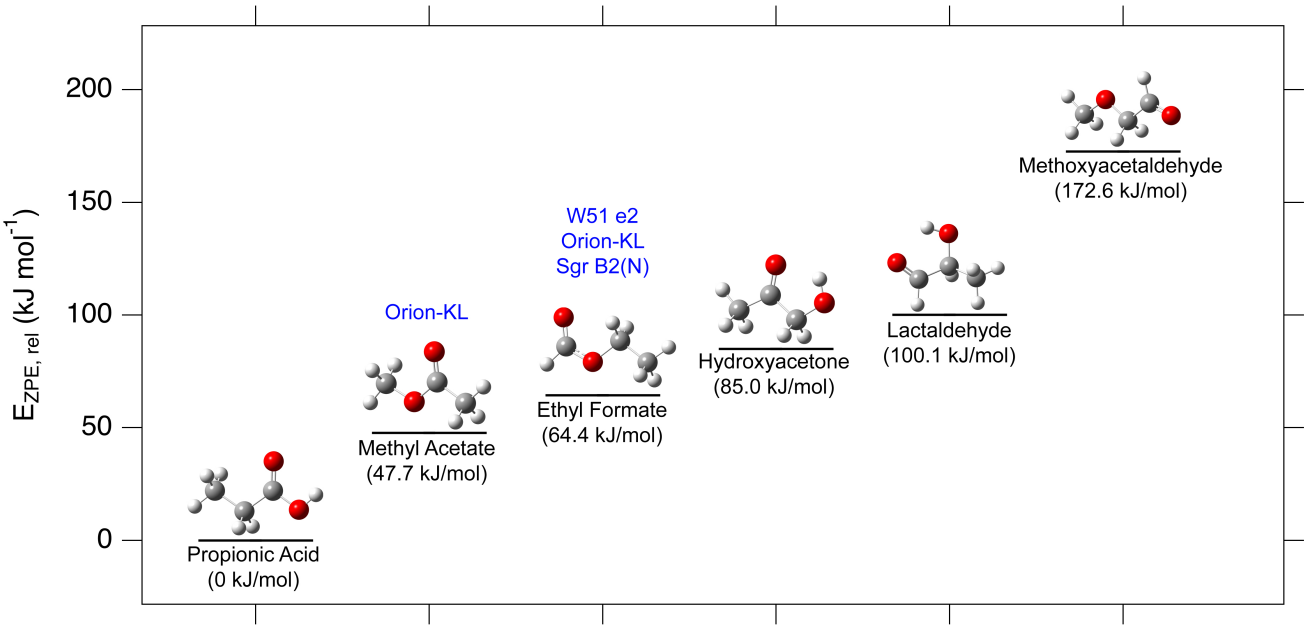

Figure 1. Relative energy ordering and structures of the six members of the $[C_3,H_6,O_2]$ isomeric family considered here. Structures and zero-point corrected energies were computed at the MP2/6-311++G(d,p) level of theory and basis set. Sources with literature detections of the molecules are displayed in blue above each (see text).

sequent functionalization yielding glyceraldehyde. Although the chemical pathways themselves are unlikely to actually proceed in such a direct fashion, the building up of complexity through the addition of small substituents on the icy surfaces of interstellar dust grains is thought to be one of the primary sources of these large (by ISM standards) organic molecules (Garrod 2013). Thus, while a set of molecules related by the addition or absence of a functional group may not be directly chemically related, they have the potential to provide unique insights into the actions of small functional groups on grain surfaces.

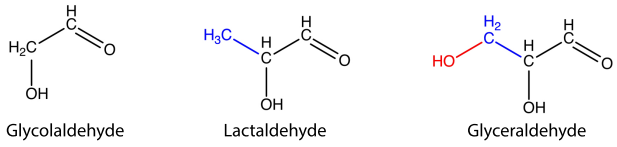

Figure 2. Structures of glycolaldehyde, lactaldehyde, and glyceraldehyde showing the underlying similarity. The glycolaldehyde backbone remains black in the lactaldehyde and glyceraldehyde structures, while the additional functional groups in each species are color coded for emphasis.

Further increasing the appeal of the molecule as an astronomical target, lactaldehyde is an active component of biological processes on Earth. These roles include a number of metabolic pathways, including pyruvate metabolism (a source of energy during exercise), as well as being involved in the production of lactic acid in a variety of conditions (Vogel et al. 2016; Sridhara & Wu 1969). It is also one of the simpler chiral molecules – those species whose mirror images are non-superimposable on each other – of which only one other such species has been detected in the ISM to date: propylene oxide (McGuire et al. 2016).

Here, we present a combined laboratory spectroscopic investigation of, and observational search for, lactaldehyde. The microwave, millimeter, and sub-millimeter wave spectra are presented and analyzed from laboratory investigations up to 460 GHz and assigned based on accompanying quantum chemical calculations. Using these assignments, we search for and report upper limits on lactaldehyde toward three high-mass star-forming regions (HMSFRs; Sgr B2(N), Orion-KL, and NGC 6334 I) and sources from the publicly available ASAI Large Project from centimeter to sub-millimeter wavelengths using a range of facilities.

2. LABORATORY SPECTROSCOPY

2.1. *Chemical Synthesis*

DL-Lactaldehyde ((R,S)-2-hydroxypropanal) was synthesized in a three-step reaction starting from 1,1-dimethoxy-2-propanone, which was then reduced to 1,1-dimethoxy-2-propanol following the procedure of Denmark & Yang (2002). The resulting alcohol was used to prepare the DL-Lactaldehyde following the ex-

perimental procedure of Hough & Jones (1952) with the dibutylacetal derivative as starting compound. In our experiments starting from the dimethyl acetal, the concentrated mixture was kept for weeks in the refrigerator before obtaining the dimer as a crystallized compound (Takahashi et al. 1983).

2.2. *Rotational Spectra Measurements*

Lactaldehyde exists predominantly as a dimer in the solid phase, and its structure has been well characterized by H-NMR, Raman an IR spectroscopy (Takahashi et al. 1983). To our knowledge, no experimentally determined structures exist for the lactaldehyde monomer, however. We have been able to release the monomer into the gas phase by heating the crystallized dimer. To do so, a small amount of solid (0.5 g) was introduced in a single neck round bottom flask connected directly to the free space cell (360 cm long Pyrex cell with an inner diameter of 10 cm and Teflon windows) of the spectrometer. The flask was evacuated ($<10^{-2}$ mbar) and then was slowly heated with a heat gun up to a temperature of 160°C of the heated air. The purity of the resulting gas-phase monomer was quite high (>95%). Above this temperature, the hydroxyacetone isomer, formed by rearrangement of the lactaldehyde, was also observed in the gaseous flow.

The optical path length of the spectrometer was doubled using a rooftop mirror and a polarization grid. The sample was continuously flowed through the cell, and an optimum gas pressure of about 25 μbar was maintained that allowed us to record the room-temperature spectra in the millimeter and sub-millimeter wave region from 80 to 460 GHz. The millimeter wave absorption spectrometer built in Universidad de Valladolid (Daly et al. 2014) is based on cascaded multiplication of the output of an Agilent E8257D microwave synthesizer (up to 20 GHz) by a set of active and passive multipliers. In this experiment, to cover the recorded spectral range, amplifier-multiplier chains WR10.0, WR6.5, and WR9.0 (VDI, Inc) in combination with an additional frequency doublers and tripler (WR2.2, WR4.3, WR2.8, VDI, Inc.) were employed. The output of the synthesizer was frequency modulated at f=10.2 kHz with modulation depth between 30 and 40 kHz. After the second pass through the cell, the signal was detected using either solid-state zero-bias detectors or a broadband quasioptical detector (VDI, Inc) and was then sent to a phase sensitive lock-in amplifier with *2f* demodulation (time constant 30 ms), resulting in a second derivative line shape. Transition frequencies were measured using a Gaussian profile function with the AABS package (Kisiel et al. 2005), which provided an accuracy better than 50 kHz for clean, unblended signals.

3. QUANTUM CHEMICAL CALCULATIONS

Because there was no previous information about lactaldehyde monomeric form, it was necessary to carry out computational calculations to support the analysis of the spectrum. The conformational space of lactaldehyde was explored using the molecular mechanics method with MMFFs force fields, obtaining three possible stable conformations for lactaldehyde (Figure 3).

The most stable one (Conformer A) is over stabilized by the *cis* disposition of the hydroxyl and carbonyl groups favoring intramolecular hydrogen bonding. The other two conformers have *trans* (Conformer B) and *cis* (Conformer C) configurations respectively with the hydroxyl group pointing away from the aldehyde group. For the geometry optimization both DFT and *ab initio* methods were employed using Gaussian 09 (Frisch et al. 2009). The model of choices were the B3LYP density functional (Becke 1992, 1993) including the Grimme D3 dispersion interactions (Grimme et al. 2010) with Becke-Johnson damping (Grimme et al. 2011) and Møller-Plesset second-order method (MP2) (Møller & Plesset 1934) and both with the Pople split-valence triple-zeta basis set augmented with diffuse and polarization functions on all atoms (the 6-311++G (d,p) basis set) (Frisch et al. 1984). The calculated values for all three conformers, including rotational constants, dipole moments, and relatively energies, are reported in Table 1, along with the experimentally determined constants for comparison.

4. ROTATIONAL SPECTRUM ANALYSIS AND ASSIGNMENT

The most stable conformer of lactaldehyde is a prolate asymmetric rotor (κ=-0.60) with symmetry properties described by the C_1 point group and values of the electric dipole moment components predicted as $|\mu_a|$=0.9, $|\mu_b|$=2.2, $|\mu_c|$=1.0 D. A portion of the room-temperature millimeter wave spectrum is illustrated in Figure 4(a). Dominant features of the spectrum are pairs of intense b-type R-branch transitions $(J+1)_{1,J+1} \leftarrow J_{0,J}$ and $(J+1)_{0,J+1} \leftarrow J_{1,J}$, which stand out above the rest. They are separated about 6.3 GHz which matches approximately with the $2C$ value predicted for the most stable *cis* conformer. These pairs are interspersed by other pairs of weaker a-type R-branch transitions $(J+1)_{0,J+1} \leftarrow J_{0,J}$ and $(J+1)_{1,J+1} \leftarrow J_{1,J}$. As J increases, the rotational energy levels with the lowest K_a quantum numbers become near-degenerate, and pairs of b-type transitions of similar intensity form quartets (see

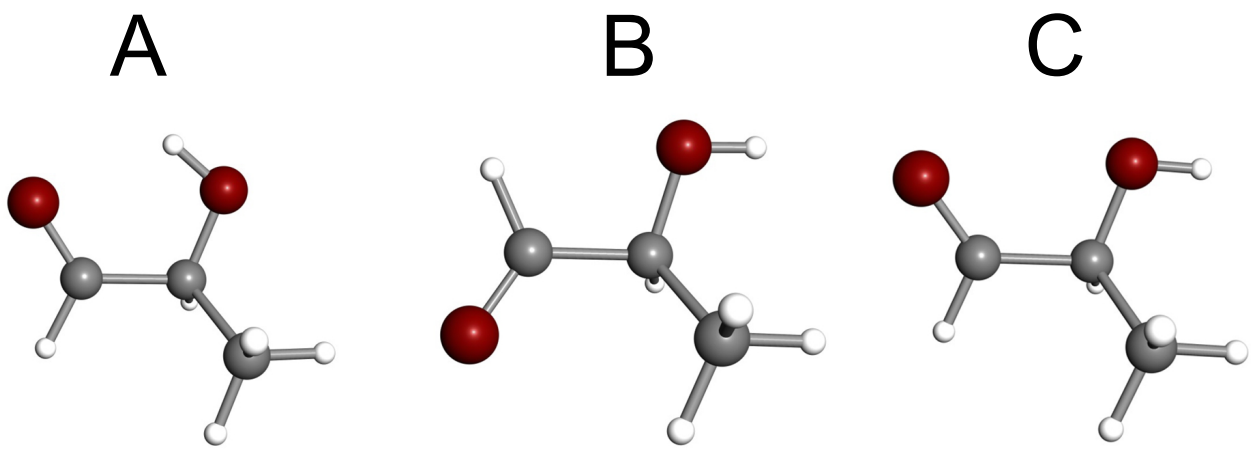

Figure 3. Three lowest-energy conformers of lactaldehyde. Conformer A has a *cis*-conformation, with a hydrogen bonding interaction between the hydroxyl and carbonyl groups, where as conformers B and C do not have this hydrogen bond.

Table 1. Experimentally determined rotational constants and comparison to the predicted rotational constants for the most stable conformers of lactaldehyde. Calculated relative energies for each conformer are also provided.

			Conformer A		Conformer B		Conformer C	
Constant	Unit	Experimental[a]	MP2	B3LYP	MP2	B3LYP	MP2	B3LYP
A	MHz	8433.0743(2)	8494.4	8438.2	8441.0	8347.1	8416.3	8170.0
B	MHz	4237.23377(6)	4213.6	4218.5	4011.1	4041.8	4192.9	4163.2
C	MHz	3145.21398(8)	3133.2	3129.7	2923.9	2916.2	3119.5	3082.1
μ_a	Debye	–	-0.9	-1.2	2.7	2.9	-3.7	-3.9
μ_b	Debye	–	-2.2	-2.2	0.9	0.7	-1.8	-1.7
μ_c	Debye	–	1.0	1.0	0.6	0.9	1.4	1.5
ΔE [b]	cm^{-1}	–	0	0	902	1032.2	1776.4	1967.5
ΔE_{ZPE}	cm^{-1}	–	0	0	779.1	900.3	1699.8	1864.7
ΔG	cm^{-1}	–	0	0	527.0	667.0	1642.8	1763.0

[a]The numbers in parentheses are 1σ uncertainties in units of the last decimal digit.
[b]ΔE and ΔG are the relative and Gibbs energies (in cm^{-1}) at 298 K with respect to the global minimum.

Fig 4b) with corresponding pairs of a-type transitions before they blend into one quadruply degenerate line. In the high-frequency side of these $K_a = 0$, 1 pair, and separated about 4.8 GHz, an analogous set of overlapped transitions corresponding to $K_a = 1$ and 2 was also identified (see also Fig.4b). Subsequently, higher K_a R-branch transitions together with several Q-branch transitions were assigned.

Finally, a total of 3023 distinct frequency lines were measured in the spectrum being assigned to a total of 5125 transitions **up to $J = 78$ and $K_a = 27$** , which correspond to 1580 b-type and 114 c-type Q-branch transition and 1495 b-type, 459 c-type and 1477 a-type R-branch transitions. The fits and predictions were made in terms of Watson's A-reduced Hamiltonian in the I^r-representation (Watson 1977) with the Pickett's SPFIT/SPCAT program suite (Pickett 1991). The present data allowed determination of the rotational constants and the full set of quartic and sextic and four octic centrifugal distortion constants listed in Table 2. The experimental values of the rotational constants match unequivocally with those predicted for the most stable *cis* conformer of lactaldehyde. The precise spectroscopic parameters derived from the analysis of the millimeter and submillimeter wave spectra enable the search of this molecule in different regions of the interstellar medium.

5. OBSERVATIONAL ANALYSIS

We have conducted a search for lactaldehyde in our own and archival spectral line observations of three

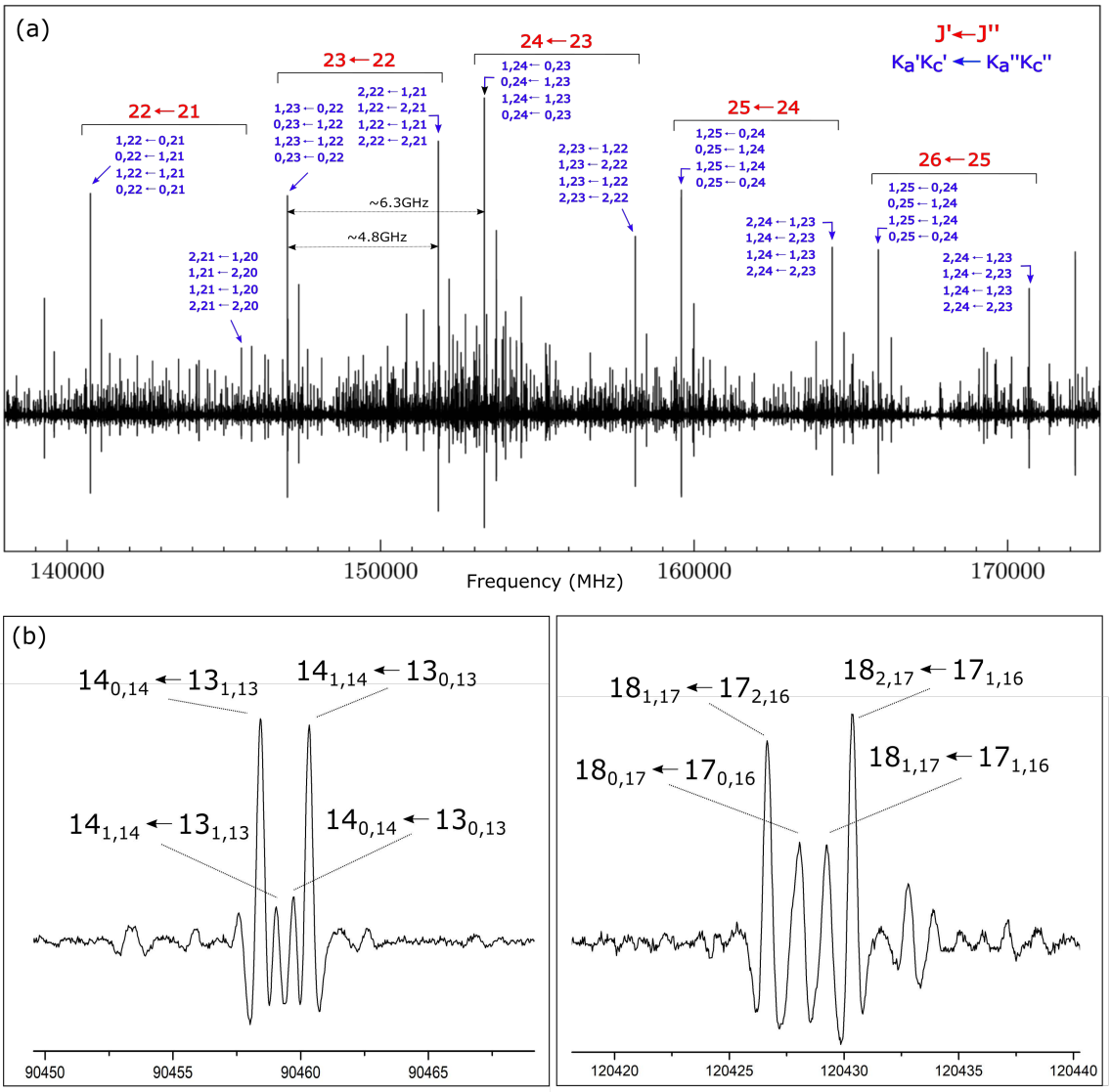

Figure 4. (a) Section of the lactaldehyde rotational spectrum with the assignment of the strongest b-type R-branch transitions.(b) Quadruplets of b-type and a-type R-branch rotational transitions of K_a= 0,1,2 values for the lowest J" values.

molecularly rich sources: NGC 6334I (MM1), Sgr B2(N), and Orion-KL, as well as in the publicly available spectra from the Astrochemical Surveys at IRAM (ASAI) Large Project.[1] For NGC 6334I (MM1), Sgr B2(N), and Orion-KL, observational details and some representative spectra are provided in the following sections. For the ASAI sources, details can be found in Lefloch et al. (2018). The ASAI sources sample a range of solar-type protostellar sources from dark clouds to Class 0/1 protostars, including shocked outflows. The spectral coverage varies from source to source, however, given the range of reasonable excitation temperatures in these sources (∼10–60 K), the strongest lines are well-covered in the data at ∼3 mm.

In all cases, the source- and molecule-specific physical parameters used to derive column densities in each source are provided in Tables 3 and 4. Column densities were calculated assuming a single-excitation temperature model following the formalisms of Hollis et al. (2004a) using Equation 1 below. If necessary, corrections due to optical depth as described in Turner (1991) would be applied. For the upper-limits reported here, $\tau \ll 1$.

[1] http://www.oan.es/asai/

$$N_T = \frac{1}{2}\frac{3k}{8\pi^3}\sqrt{\frac{\pi}{\ln 2}}\frac{Qe^{E_u/T_{\rm ex}}\Delta T_b \Delta V}{B\nu S_{ij}\mu^2}\frac{1}{1-\frac{e^{h\nu/kT_{\rm ex}}-1}{e^{h\nu/kT_{\rm bg}}-1}} \quad (1)$$

Table 2. Ground State Spectroscopic Constants of Lactaldehyde

Constant	Unit	Exp. value[a]	**Theor. value**[b]
A	MHz	8433.07428(18)	**8438.2**
B	MHz	4237.233774(64)	**4218.5**
C	MHz	3145.213978(77)	**3129.7**
Δ_J	MHz	0.001784714(65)	**0.002**
Δ_{JK}	MHz	−0.00209014(21)	**−0.003**
Δ_K	MHz	0.01782873(73)	**0.02**
δ_J	kHz	0.304926(10)	**0.3**
δ_k	kHz	2.57516(14)	**2.0**
Φ_{JK}	mHz	−6.94(10)	
Φ_{KJ}	mHz	−98.38(52)	
Φ_J	mHz	4.466(23)	
Φ_K	mHz	112.2(10)	
ϕ_J	mHz	0.8170(20)	
ϕ_{JK}	mHz	8.712(46)	
ϕ_K	mHz	5.61(23)	
L_J	mHz	−0.0000183(27)	
L_{JJK}	mHz	−0.000364(19)	
L_{JK}	mHz	0.00377(16)	
L_{KKJ}	mHz	−0.00935(63)	
$\sigma_{\rm fit}$ [c]	kHz	33	

[a]The numbers in parentheses are 1σ uncertainties in units of the last decimal digit.
[b]B3LYP/GD3BJ
[c]Root mean square deviation of the fit.

Here, N_T is the total column density (cm^{-1}), Q is the partition function, T_{ex} is the excitation temperature (K), E_u is the upper state energy (K), ΔT_b is the peak intensity (K), ΔV is the full-width at half-maximum of the line (km s^{-1}), B is the beam filling factor, ν is the frequency (Hz), S_{ij} is the intrinsic quantum mechanical line strength, μ is the permanent dipole moment (Debye[2]), and T_{bg} is the background continuum temperature (K). For the upper-limits presented here, a simulated spectrum was generated using the parameters described for each observation below. The strongest predicted line that was absent from the observational spectrum was then chosen and used to calculate the 1σ upper limit, taking the rms noise value at that point as the value of the brightness temperature ΔT_b.

For each molecule, the rotational component of the partition function was calculated by direct state counting over all states i using Equation 2 (c.f. Gordy & Cook 1984).

$$Q_r = \sum_{i=0}^{\infty} (2J+1) e^{-E_i/kT_{ex}} \quad (2)$$

We have also computed the vibrational contribution to the total partition function, calculated as,

$$Q = Q_{\rm v} \times Q_{\rm r} \quad (3)$$

$$Q_{\rm v} = \prod_{i=1}^{3N-6} \frac{1}{1 - e^{-E_i/kT_{\rm ex}}} \quad (4)$$

summing over all quanta in all vibrational states. The harmonic energies of these states were calculated using Gaussian 16 at the MP2/6-311++G(d,p) level of theory and basis set.

In all cases, a single transition was selected to perform the non-detection upper limit analysis. The transition was selected to be the strongest transition at the given excitation temperature that had the least overlap with interfering lines. This provided the most stringent upper limit possible given the available observations.

5.1. *NGC 6334I (MM1)*

NGC 6334I is a nearby HMSFR located at a heliocentric distance of 1.3 kpc as measured by maser parallax (Chibueze et al. 2014). The source displays extensive substructure, with the two primary targets for molecular study designated MM1 and MM2, separated by only ∼2000 au, the former of which is the larger and may have multiple embedded protostars (Brogan et al. 2018; Hunter et al. 2018). MM1 in particular has been shown to be extremely molecularly rich, including providing the first interstellar detection of methoxymethanol (CH_3OCH_2OH; McGuire et al. 2017, 2018b).

The observations toward NGC 6334 I (MM1) were obtained with the Atacama Large Millimeter/submillimeter Array (ALMA) during Cycle 3 (2016) and were calibrated using the ALMA Cycle 4 pipeline (CASA 4.7.2). Full details are described in Hunter et al. (2017), McGuire et al. (2017), and Brogan et al. (2018). Briefly, the phase-center of the observations was at (J2000) α=17:20:53.36, δ= −35:47:00.0. The angular resolution was convolved to $0.26''\times0.26''$ for uniformity as part of an unrelated analysis. A total of 15 GHz of spectra in Band 7 in two frequency ranges were obtained, centered at 287 GHz and 344 GHz. The spectral resolution was 1.1 km s^{-1} with an rms per channel noise of 2.0 mJy beam^{-1} (287 GHz) and 3.3 mJy beam^{-1} (344 GHz). For the analysis presented here, we assumed physical parameters (Table 4) to match those

[2] Care must be taken to convert this unit for compatibility with the rest of the parameters.

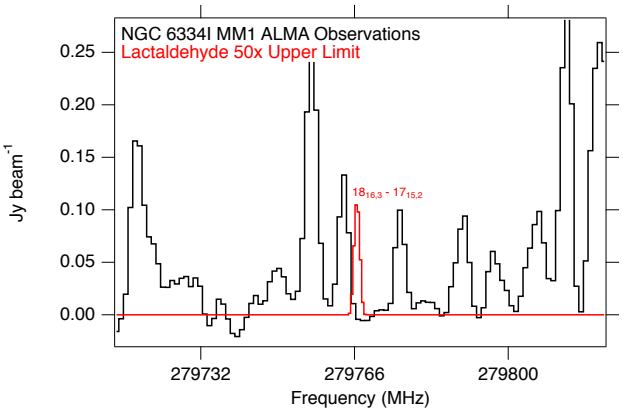

Figure 5. ALMA observations toward NGC 6334I (MM1) in black, with a simulation of lactaldehyde emission overlaid in red and multiplied by 50 to show detail. The simulation was performed using the parameters given in Table 4.

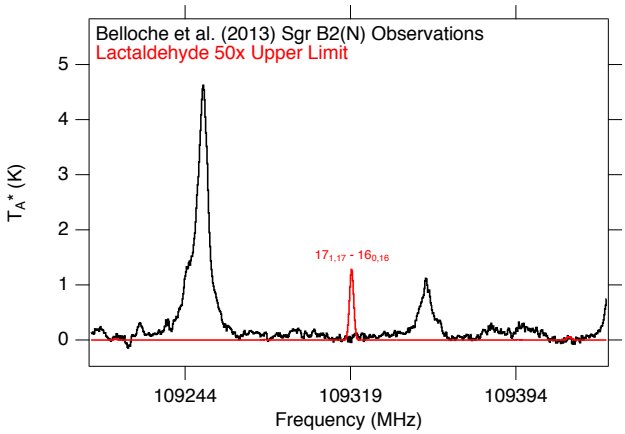

Figure 6. IRAM 30-m observations toward Sgr B2(N) in black from Belloche et al. (2013), with a simulation of lactaldehyde emission overlaid in red and multiplied by 50 to show detail. The simulation was performed using the parameters given in Table 4.

derived for glycolaldehyde in this source by McGuire et al. (2018b). The spectra toward NGC 6334I (MM1) used to derive the upper limit, as well as the transition detailed in Table 4, are shown in Figure 5.

5.2. *Sgr B2(N)*

Sgr B2(N) is the pre-eminent source for new detections of complex organic molecules in the ISM, with almost half (32 out of 70) of all first detections of carbon-bearing molecules of six or more atoms occurring in this source (McGuire 2018). Located at a distance of 8.3 kpc (Reid et al. 2014), the complex contains a number of embedded molecular cores separated by of order a few arcseconds (see, e.g., Belloche et al. 2016). Most molecules are detected either with warm temperatures in relatively compact distributions around the cores, or with sub-thermal excitation conditions in a cold, diffuse shell surrounding the complex (McGuire et al. 2016).

Two datasets toward Sgr B2(N) were examined: the IRAM 30-m 80–116 GHz survey of Belloche et al. (2013) and the *Herschel* Observations of EXtraordinary Sources (HEXOS) key project Band 1a (480–560 GHz) survey presented in Neill et al. (2014).

5.2.1. *Belloche et al. (2013) 80–116 GHz Survey*

Details of these observations are presented in Belloche et al. (2013). The spectra presented here were obtained with the IRAM 30-m telescope in 2004 and 2005. The pointing position was (J2000) α=17:47:20.0, δ=28:22:19.0. The spectra used here between 80–116 GHz have a spectral resolution of 312.5 kHz and a median rms per channel noise level of ∼13–43 mK across the spectrum. For the analysis presented here, we chose physical parameters (Table 4) to match those of glycolaldehyde from the Belloche et al. (2013) survey. The spectra toward Sgr B2(N) used to derive the upper limit, as well as the transition detailed in Table 4, are shown in Figure 6.

5.2.2. *HEXOS 480–560 GHz Survey*

Details of the observations are presented in Neill et al. (2014). The spectra presented here were taken with the Heterodyne Instrument for the Far-Infrared (HIFI) spectrometer (de Graauw et al. 2010) onboard the *Herschel Space Observatory* (Pilbratt et al. 2010). Despite being the source of the first interstellar detection of glycolaldehyde (Hollis et al. 2000), the molecule was not detected in the HEXOS survey of the source Neill et al. (2014), perhaps due to substantial beam dilution effects (a ∼4″ source in a ∼40″ beam at the lowest frequencies). Here, we have therefore used the physical parameters (Table 4) of dimethyl ether (CH_3OCH_3) in our calculations. The spectra have an rms noise value of 15 mK and a resolution of 500 kHz. The spectra toward Sgr B2(N) used to derive the upper limit, as well as the transition detailed in Table 4, are shown in Figure 7.

5.3. *Orion-KL*

At a distance of 414±7 pc (Menten et al. 2007), Orion-KL is the closest of the HMSFRs studied here. Like Sgr B2(N), it has been the sight of numerous new molecular detections; while only six carbon-containing COMs were identified in Orion-KL for the first time, a total of 25 species (12%) of all first detections occurred in the source (McGuire 2018). Like both NGC 6334I and Sgr B2(N), Orion-KL displays substantial physical substructure, with the primary components being designated the hot core and compact ridge, with associated high and low velocity outflows and an extended molecular ridge

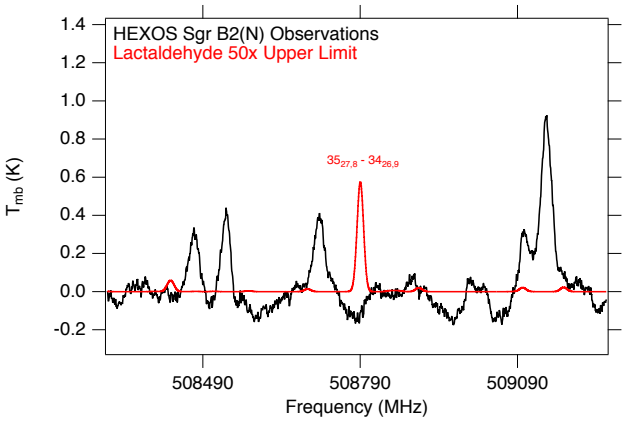

Figure 7. Observations toward Sgr B2(N) in black from the *Herschel* HEXOS key project (Neill et al. 2014), with a simulation of lactaldehyde emission overlaid in red and multiplied by 50 to show detail. The simulation was performed using the parameters given in Table 4.

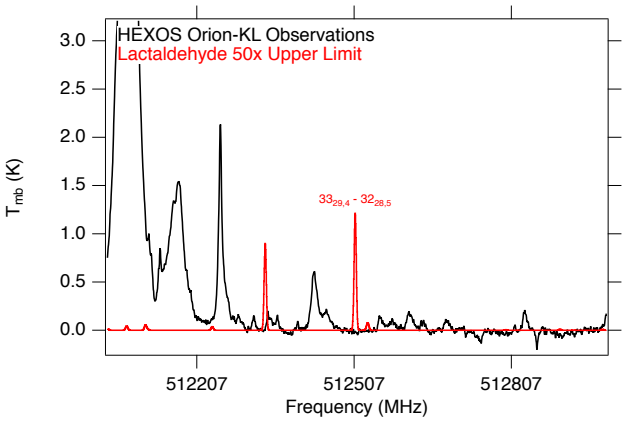

Figure 8. Observations toward Orion-KL in black from the *Herschel* HEXOS key project (Crockett et al. 2014), with a simulation of lactaldehyde emission overlaid in red and multiplied by 50 to show detail. The simulation was performed using the parameters given in Table 4.

some distance from the cores (see Figure 7 of Crockett et al. 2014). The observations used here are also from the *Herschel* HEXOS key project, obtained with the HIFI instrument. The observational and data reduction details are described in Crockett et al. (2014). As with the HEXOS observations of Sgr B2(N), there was no reported detection of glycolaldehyde, and so we have adopted the physical parameters of (Table 4) CH_3OCH_3 for this study. The spectra have an rms noise level of 20 mK and a resolution of 500 kHz. The spectra toward Orion-KL used to derive the upper limit, as well as the transition detailed in Table 4, are shown in Figure 8.

6. DISCUSSION

Table 3. Source parameters assumed in each of the sets of observations.

Source	Telescope	θ_s^a ($''$)	T_{bg} (K)	ΔV (km s^{-1})	$T_b^\dagger$ (mK)	T_{ex} (K)	Refs.
NGC 6334I	ALMA	–	33.9	3.2	1[b]	135	1
Sgr B2(N)	IRAM	10	5.2	6.0	22	80	2
Sgr B2(N)	*Herschel*	3.7	5.2	8.5	30	130	3
Orion-KL	*Herschel*	10	4.4	2.8	22	110	4
Barnard 1	IRAM	–	2.7	0.8	4.6	10	5, 6
IRAS 4A	IRAM	–	2.7	5.0	2.3	21	5, 7
L1157B1	IRAM	–	2.7	8.0	2.2	60	8
L1157mm	IRAM	–	2.7	3.0	2.6	60	8
L1448R2	IRAM	–	2.7	8.0	2.8	60	⋆, 9
L1527	IRAM	–	2.7	0.5	2.4	12	9, 10
L1544	IRAM	–	2.7	0.5	3.1	10	11, 12
SVS13A	IRAM	0.3	2.7	3.0	2.3	80	5, 7
TMC1	IRAM	–	2.7	0.3	11	7	13, 14

[a]Except where noted, the source is assumed to fill the beam.
[b]For these interferometric observations, the intensity is given in mJy/beam rather than mK.
†Taken either as the 1σ RMS noise level at the location of the target line, or for line confusion limited spectra, the reported RMS noise of the observations.
⋆For this shocked location within a molecular outflow, the same parameters were assumed as for L1157-B1.
References – [1] McGuire et al. 2018b [2] Belloche et al. 2013 [3] Neill et al. 2014 [4] Crockett et al. 2014 [5] Melosso et al. 2018 [6] Cernicharo et al. 2018 [7] Higuchi et al. 2018 [8] McGuire et al. 2015 [9]Jørgensen et al. 2002 [10] Araki et al. (2017) [11] Hily-Blant et al. 2018 [12] Crapsi et al. 2005 [13] McGuire et al. 2018a [14] Gratier et al. 2016

Until quite recently, it was generally thought that most molecules more complex than methanol (CH_3OH) were predominantly formed in the ISM through reaction on or within the icy mantles of dust grains (see, e.g., Herbst & van Dishoeck 2009). These environments play a number of important roles, from concentration effects to serving as third bodies to dissipate excess energy from highly exothermic reactions such as those between two radicals (e.g. Garrod 2013). These molecules are then lifted into the gas phase for detection either thermally, by the gradual warm-up of an embedded protostar in their molecular cloud (Garrod et al. 2008), or non-thermally, typically by being liberated en masse by the passage of a shock (Requena-Torres et al. 2006). Recent work, however, particularly pertaining to lactaldehyde's simpler cousin glycolaldehyde, has suggested that gas-phase production routes may be not only operable, but substantial if not dominant contributors to the observed abundance of this species in a number of sources (Skouteris et al. 2018). Indeed, the smaller $[C_2,H_4,O_2]$ isomeric family, which contains not only glycolaldehyde but also methyl formate (CH_3OCHO) and acetic acid (CH_3COOH) has long been used as a sort of test bed for competing theories of molecular evolution (see, e.g., Laas et al. 2011; Skouteris et al. 2018; Balucani et al. 2015). Because the $[C_3,H_6,O_2]$ contains a wider num-

Table 4. Upper limits and the line parameters used to calculate them in each of the sets of observations.

Source	Frequency[a] (MHz)	Transition[a] ($J'_{K_a,K_c} - J''_{K_a,K_c}$)	E_u (K)	$S_{ij}\mu^{2,\dagger}$ (Debye^2)	Q	N_T (cm^{-2})	$N(\mathrm{H_2})$ (cm^{-2})	X_{H_2}	Refs. ($N(\mathrm{H_2})$)
NGC 6334I	279766.3	$18_{16,x} - 17_{15,x}$	118.9	178.9	191444	$\leq 2 \times 10^{16}$	–	–	–
Sgr B2(N)	109319.3	$17_{x,17} - 17_{x,16}$	48.1	180.2	24453	$\leq 3 \times 10^{14}$	1×10^{24}	$\leq 3 \times 10^{-10}$	1
Sgr B2(N)	508789.9	$35_{27,x} - 34_{26,x}$	389.6	305.5	158992	$\leq 1 \times 10^{17}$	1×10^{24}	$\leq 1 \times 10^{-7}$	1
Orion-KL	512507.1	$33_{29,x} - 32_{28,x}$	390.0	329.0	75632	$\leq 3 \times 10^{15}$	3.9×10^{23}	$\leq 8 \times 10^{-9}$	2
Barnard 1	96473.8	$6_{6,x} - 5_{5,x}$	15.6	63.4	505	$\leq 4 \times 10^{11}$	1.5×10^{23}	$\leq 3 \times 10^{-12}$	3
IRAS 4A	103033.0	$16_{x,16} - 15_{x,15}$	42.9	168.8	1562	$\leq 1 \times 10^{12}$	3.7×10^{23}	$\leq 3 \times 10^{-12}$	3
L1157B1	103033.0	$16_{x,16} - 15_{x,15}$	42.9	168.8	11149	$\leq 4 \times 10^{12}$	1×10^{21}	$\leq 4 \times 10^{-9}$	3
L1157mm	103033.0	$16_{x,16} - 15_{x,15}$	42.9	168.8	11149	$\leq 2 \times 10^{12}$	6×10^{21}	$\leq 3 \times 10^{-10}$	3
L1448R2	103033.0	$16_{x,16} - 15_{x,15}$	42.9	168.8	11149	$\leq 5 \times 10^{12}$	3.5×10^{23}	$\leq 1 \times 10^{-11}$	4
L1527	103912.0	$7_{6,x} - 6_{5,x}$	18.1	63.1	664	$\leq 3 \times 10^{11}$	2.8×10^{22}	$\leq 1 \times 10^{-11}$	4
L1544	96473.8	$6_{6,x} - 5_{5,x}$	15.6	63.4	505	$\leq 2 \times 10^{11}$	5×10^{21}	$\leq 4 \times 10^{-11}$	5
SVS13A	96473.8	$11_{9,x} - 10_{8,x}$	41.9	97.8	24453	$\leq 2 \times 10^{16}$	3×10^{24}	$\leq 7 \times 10^{-9}$	6
TMC1	130188.5	$8_{8,x} - 7_{7,x}$	27.3	86.74	296	$\leq 1 \times 10^{12}$	1×10^{22}	$\leq 1 \times 10^{-10}$	3

[a]These transitions have un-resolved K-splitting at the linewidths of the sources under consideration.
[†]Sum of the values for the unresolved, K-split lines.
References – [1] Lis & Goldsmith 1990 [2] Crockett et al. 2014 [3] Cernicharo et al. 2018 [4] Jørgensen et al. 2002 [5] Vastel et al. 2014 [6] Chen et al. 2009

ber of reasonable interstellar candidates, with a larger array of functional groups, it could conceivably serve as an analogous probe of the next level in evolutionary complexity.

As we have shown here, however, detecting the various members of this family continues to prove challenging. From a purely thermodynamical viewpoint, it might not be surprising that lactaldehyde is not detected if the next lowest member, hydroxyacetone, is not either. There are issues with this particular argument, however. First, is that this *Minimum Energy Principle*, in which the lowest-energy isomer of a family is assumed to be the most abundant, is not generally applicable, and we must consider the influence of reaction kinetics on abundances (Loomis et al. 2015). Indeed, while both methyl acetate and ethyl formate are detected in space, the lowest-energy isomer, propionic acid, has not been reported thus far (McGuire 2018). Second, even if we are to assume that a molecule such as lactaldehyde is less abundant than a lower-energy species, differences in the strength of the rotational spectra, complexity from internal motions, and partition functions between two species can play a major role in the detectability.

All that said, the fact that there is such a disparity in the detection rates, and the derived abundances and upper limits, could provide some stringent constraints on the possible formation and destruction pathways that dominate the chemistry of this family. Doing so will likely first require a dedicated observational effort to uniformly observe this family across a wide sample of sources. While many observational sets, such as those used here, do exist and cover favorable transitions for many of these species, they are largely taken with a range of facilities, and at differing resolutions and sensitivities, making it difficult to arrive at a homogenous dataset. The ASAI dataset does provide this sort of uniform coverage, but does not include examples of the high-mass star-forming regions where methyl acetate and ethyl formate have been so far detected. Further hindering this effort is a lack of laboratory spectra of propionic acid above ∼100 GHz.

Dedicated efforts to model the formation chemistry of the family as a whole will also be required. Many of the molecules have had their formation and destruction pathways investigated to various degrees individually. For example, Peng et al. (2019) propose a number of mechanisms for ethyl formate, and Belloche et al. (2009) incorporate ethyl formate chemistry into the model of Garrod et al. (2008). Yet, to our knowledge, no model has examined the chemistry of this family as a whole. Such a complete study might yield insights into the continued non-detection of these species other than ethyl formate and methyl acetate.

7. CONCLUSIONS

Precise ground state spectroscopic constants up to octic centrifugal distortion constants for the monomeric form of lactaldehyde are provided in the present work. New direct laboratory data allowed to search for the lactaldehyde in three high-mass star-forming regions (NGC 6334I, Sgr B2(N), and Orion-KL) and sources from the ASAI Large Project. Although no spectral features of lactaldehyde were found, present data can be used with

confidence in future searches for lactaldehyde in other interstellar sources.

The research leading to these results has received funding from the European Research Council under the European Union's Seventh Framework Programme (FP/2007-2013)/ ERC-2013-SyG, grant agreement No. 610256 NANOCOSMOS, Ministerio de Ciencia e Innovación (Grants CTQ2013-40717-P, CTQ2016-76393-P), and Junta de Castilla y León (grants VA175U13 and VA077U16). E.R.A. thanks Ministerio de Ciencia e Innovación for a FPI grant (BES-2014-067776). B.A.M. thanks K.L.K. Lee for helpful quantum chemical discussions and G.A. Blake for access to computing resources. This manuscript makes use of the following ALMA data: ADS/JAO.ALMA#2015.A.00022.T and #2017.1.00717.S. ALMA is a partnership of ESO (representing its member states), NSF (USA) and NINS (Japan), together with NRC (Canada) and NSC and ASIAA (Taiwan) and KASI (Republic of Korea), in cooperation with the Republic of Chile. The Joint ALMA Observatory is operated by ESO, AUI/NRAO and NAOJ. The National Radio Astronomy Observatory is a facility of the National Science Foundation operated under cooperative agreement by Associated Universities, Inc. Support for B.A.M. was provided by NASA through Hubble Fellowship grant #HST-HF2-51396 awarded by the Space Telescope Science Institute, which is operated by the Association of Universities for Research in Astronomy, Inc., for NASA, under contract NAS5-26555. J.C.G. received funding support from the Centre National d'Etudes Spatiales (CNES) and the French Programme National "Physique et Chimie du Milieu Interstellaire.

REFERENCES

Apponi, A. J., Hoy, J. J., Halfen, D. T., Ziurys, L. M., & Brewster, M. A. 2006, The Astrophysical Journal, 652, 1787

Araki, M., Takano, S., Sakai, N., et al. 2017, The Astrophysical Journal, 847, 0

Balucani, N., Ceccarelli, C., & Taquet, V. 2015, Monthly Notices of the Royal Astronomical Society: Letters, 449, L16

Becke, A. D. 1992, The Journal of Chemical Physics, 96, 2155

—. 1993, The Journal of Chemical Physics, 98, 1372

Belloche, A., Garrod, R. T., Müller, H. S. P., et al. 2009, A&A, 499, 215

Belloche, A., Müller, H. S. P., Garrod, R. T., & Menten, K. M. 2016, A&A, 587, A91

Belloche, A., Müller, H. S. P., Menten, K. M., Schilke, P., & Comito, C. 2013, A&A, 559, A47

Brogan, C. L., Hunter, T. R., Cyganowski, C. J., et al. 2018, The Astrophysical Journal, 866, 87

Cernicharo, J., Lefloch, B., Agúndez, M., et al. 2018, The Astrophysical Journal Letters, 853, L22

Chen, X., Launhardt, R., & Henning, T. 2009, The Astrophysical Journal, 691, 1729

Chibueze, J. O., Omodaka, T., Handa, T., et al. 2014, The Astrophysical Journal, 784, 114

Crapsi, A., Caselli, P., Walmsley, C. M., et al. 2005, The Astrophysical Journal, 619, 379

Crockett, N. R., Bergin, E. A., Neill, J. L., et al. 2014, The Astrophysical Journal, 787, 112

Daly, A., Kolesniková, L., Mata, S., & Alonso, J. 2014, Journal of Molecular Spectroscopy, 306, 11

de Graauw, T., Helmich, F. P., Phillips, T. G., et al. 2010, A&A, 518, L6

Denmark, S. E., & Yang, S.-M. 2002, Journal of the American Chemical Society, 124, 2102, pMID: 11878949

Frisch, M. J., Pople, J. A., & Binkley, J. S. 1984, The Journal of Chemical Physics, 80, 3265

Frisch, M. J., Trucks, G. W., Schlegel, H. B., et al. 2009, Gaussian 09, Revision D.01, Gaussian, Inc., Wallingford CT

Garrod, R. T. 2013, The Astrophysical Journal, 765, 60

Garrod, R. T., Weaver, S. L. W., & Herbst, E. 2008, Astrophys. J., 682, 283

Gordy, W., & Cook, R. L. 1984, Microwave Molecular Spectra, 3rd edn. (New York: Wiley)

Gratier, P., Majumdar, L., Ohishi, M., et al. 2016, The Astrophysical Journal Supplement Series, 225, 1

Grimme, S., Antony, J., Ehrlich, S., & Krieg, H. 2010, The Journal of Chemical Physics, 132, 154104

Grimme, S., Ehrlich, S., & Goerigk, L. 2011, Journal of Computational Chemistry, 32, 1456

Herbst, E., & van Dishoeck, E. F. 2009, Annual Reviews of Astronomy and Astrophysics, 47, 427

Higuchi, A. E., Sakai, N., Watanabe, Y., et al. 2018, The Astrophysical Journal Supplement Series, 236, 0

Hily-Blant, P., Faure, A., Vastel, C., et al. 2018, Monthly Notices of the Royal Astronomical Society, 480, 1174

Hollis, J. M., Jewell, P. R., Lovas, F. J., & Remijan, A. 2004a, The Astrophysical Journal, 613, L45

Hollis, J. M., Jewell, P. R., Lovas, F. J., Remijan, A., & Møllendal, H. 2004b, The Astrophysical Journal, 610, L21
Hollis, J. M., Lovas, F. J., & Jewell, P. R. 2000, The Astrophysical Journal, 540, L107
Hough, L., & Jones, J. K. N. 1952, Journal of the Chemical Society, 4052
Hunter, T. R., Brogan, C. L., MacLeod, G., et al. 2017, The Astrophysical Journal Letters, 837, L29
Hunter, T. R., Brogan, C. L., MacLeod, G. C., et al. 2018, The Astrophysical Journal, 854, 0
Jaman, A. I., Chakraborty, S., & Chakraborty, R. 2015, Journal of Molecular Structure, 1079, 402
Jørgensen, J. K., Schöier, F. L., & van Dishoeck, E. F. 2002, A&A, 389, 908
Kisiel, Z., Pszczółkowski, L., Medvedev, I. R., et al. 2005, Journal of Molecular Spectroscopy, 233, 231 , http://www.ifpan.edu.pl/~kisiel/aabs/aabs.htm#aabs
Kolesniková, L., Peña, I., Alonso, E. R., et al. 2018, A&A, 619, A67
Laas, J. C., Garrod, R. T., Herbst, E., & Widicus Weaver, S. L. 2011, The Astrophysical Journal, 728, 71
Lefloch, B., Bachiller, R., Ceccarelli, C., et al. 2018, Monthly Notices of the Royal Astronomical Society, 477, 4792
Lis, D. C., & Goldsmith, P. F. 1990, The Astrophysical Journal, 356, 195
Loomis, R. A., McGuire, B. A., Shingledecker, C., et al. 2015, The Astrophysical Journal, 799, 34
McGuire, B. A. 2018, The Astrophysical Journal Supplement Series, 239, 17
McGuire, B. A., Burkhardt, A. M., Kalenskii, S. V., et al. 2018a, Science, 359, 202
McGuire, B. A., Carroll, P. B., Loomis, R. A., et al. 2016, Science, 352, 1449
McGuire, B. A., Carroll, P. B., Dollhopf, N. M., et al. 2015, The Astrophysical Journal, 812, 1
McGuire, B. A., Shingledecker, C. N., Willis, E. R., et al. 2017, The Astrophysical Journal Letters, 851, L46
McGuire, B. A., Brogan, C. L., Hunter, T. R., et al. 2018b, The Astrophysical Journal Letters, 863, L35
Melosso, M., Melli, A., Puzzarini, C., et al. 2018, A&A, 609, A121
Menten, K. M., Reid, M. J., Forbrich, J., & Brunthaler, A. 2007, A&A, 474, 515
Møller, C., & Plesset, M. S. 1934, Physical Review, 46, 618
Neill, J. L., Bergin, E. A., Lis, D. C., et al. 2014, The Astrophysical Journal, 789, 8
Peng, Y., Rivilla, V. M., Zhang, L., Ge, J. X., & Zhou, B. 2019, The Astrophysical Journal, 871, 0
Pickett, H. M. 1991, Journal of Molecular. Spectroscopy, 148, 371 , http://spec.jpl.nasa.gov/
Pilbratt, G. L., Riedinger, J. R., Passvogel, T., et al. 2010, A&A, 518, L1
Reid, M. J., Menten, K. M., Brunthaler, A., et al. 2014, The Astrophysical Journal, 783, 130
Requena-Torres, M. A., Martin-Pintado, J., Rodríguez-Franco, A., et al. 2006, A&A, 455, 971
Skouteris, D., Balucani, N., Ceccarelli, C., et al. 2018, The Astrophysical Journal, 854, 135
Sridhara, S., & Wu, T. T. 1969, The Journal of biological chemistry, 244, 5233
Stiefvater, O. L. 1975a, The Journal of Chemical Physics, 62, 233
—. 1975b, The Journal of Chemical Physics, 62, 244
Takahashi, H., Kobayashi, Y., & Kaneko, N. 1983, Spectrochimica Acta Part A: Molecular Spectroscopy, 39, 569
Tercero, B., Kleiner, I., Cernicharo, J., et al. 2013, The Astrophysical Journal, 770, L13
Turner, B. E. 1991, The Astrophysical Journal Supplement Series, 76, 617
Vastel, C., Ceccarelli, C., Lefloch, B., & Bachiller, R. 2014, The Astrophysical Journal Letters, 795, L2
Vogel, M. A. K., Bürger, H., Schläger, N., et al. 2016, Reaction Chemistry & Engineering, 1, 156
Watson, J. K. G. 1977, in Vibrational Spectra and Structure, ed. J. R. Durig, Vol. 6 (Amsterdam: Elsevier), 1–89